CHAPTER - IV

PREPARATION AND CHARACTERIZATION OF Sb_2S_3 THIN FILMS FROM NON - AQUEOUS MEDIUM

4.1 INTRODUCTION

Recently considerable attention has been given to the preparation and characterization of metal chalcogenide films using various techniques [1 -3]. Among various metal sulphides, antimony trisulphide finds some special applications to target material of television cameras [4], microwave devices [5], switching devices [6], various optoelectronic devices [7-9] and a potential material for write once read many times (WORM) kind of storage applications [10].

Literature survey shows that Sb_2S_3 thin films deposited from an aqueous medium by chemical bath deposition and spray pyrolysis are amorphous while the electrodeposited films are polycrystalline [11-18] . Only few reports are available on the preparation of Sb_2S_3 thin films from a non-aqueous medium. In the present chapter emphasis is given on the deposition of Sb_2S_3 thin films from a non-aqueous medium and study of their structural, optical and electrical properties.

4.2 EXPERIMENTAL

Sb_2S_3 thin films have been deposited by a spray pyrolysis technique as discussed in chapter III.

4.2.1 Thin Film deposition

4.2.1.1 Substrate cleaning

The substrate cleaning procedure discussed in section 3.2.1.2 is used to clean the glass substrates.

4.2.1.2 Preparation of solutions

The initial ingredients used to prepare Sb_2S_3 thin films are as follows:

1) A.R.Grade antimony trichloride [$SbCl_3$] supplied by s.d. fine chem., Boisar, Mumbai.

2) A.R.Grade thiourea [$CS(NH_2)_2$] supplied by Loba Chemicals, Mumbai-2.

3) A.R.Grade, acetic acid (glacial) [CH_3COOH] supplied by Qualigens Fine Chemicals , Mumbai.

The solutions of antimony trichloride and thiourea were prepared by dissolving required amounts in acetic acid (glacial), a non-aqueous solvent. The equimolar solutions of $SbCl_3$ and [$CS(NH_2)_2$] were mixed together in appropriate volumes to obtain Sb:S ratio of 2:3. The mixed solutions were kept about 12 hours so that yellowish turbidity disappears and clear solution is obtained.

4.2.1.3 Deposition of Sb_2S_3 thin films

The mixed solution (20 cc) of $SbCl_3$ and [$CS(NH_2)_2$] was sprayed onto the preheated glass substrates kept at desired substrate temperature. The nozzle to substrate distance was kept to be 30 cm. When the droplets of the mixed solution reach the hot substrates, well adherent and dark gray coloured films of Sb_2S_3 are formed on the substrates.

4.2.1.4 Spray rate

The spray rate is one of the important preparative parameters in thin film deposition by the spray pyrolysis technique. The spray rate can be varied either by changing the air pressure of the carrier gas or the height of liquid level

monitor as discussed in section 3.3.1.1. During the Sb_2S_3 film deposition the spray rate was maintained to be 10 cc min^{-1}.

4.2.1.5 Substrate Temperature

The substrate temperature plays an important role in spray pyrolysis technique as it affects the crystallinity and stoichiometry of compound formation. To optimize the substrate temperature, 0.1M solutions of $SbCl_3$ and $CS(NH_2)_2$ was sprayed with spray rate of 10 cc min^{-1} onto the set of glass substrates maintained at temperatures of 240, 250 and 260^0 C. The structural and electrical analysis of these films reveals that the films deposited at 250 ^oC have relatively higher crystallinity and conductivity as compared to the films deposited at 240 ^oC and 260 ^oC. Thus 250 ^oC is fixed as the optimised temperature for film deposition.

4.2.1.6 Concentration of spraying solution

The concentration of the solution also affects to a great extent to the physical properties of spray deposited thin films. The Sb_2S_3 thin films were prepared at solution concentrations of 0.05M, 0.1M and 0.125M at optimized substrate temperature of 250^0 C. The solution concentration was optimised to be 0.1M as discussed in section 3.3.1.4.

4.2.1.7 Sb:S volume ratio

It has been found that mere change in volumetric proportion of the initial solutions for spraying can significantly affect the properties of deposited material and may be the effective method for controlling the properties of the deposited material [19]. With a view to optimize the composition (Sb:S

volume ratio), the Sb_2S_3 thin films were prepared at various volume compositions as 1:9, 2:8, 3:7, 4:6, 5:5, 6:4, 7:3, 8:2, and 9:1 of Sb:S at substrate temperature of 250 ^oC, solution concentration of 0.1 M and at spray rate of 10 cc min^{-1}. The structural and electrical characterisation shows that the films prepared at 4:6 composition have relatively higher crystallinity and conductivity. The change in the crystallinity with change in Sb:S composition may be attributed to the slight change in stoichiometric proportion in the samples during the pyrolytic decomposition of the material [20]. Thus 2:3 is the optimized composition of Sb and S for the deposition of Sb_2S_3 thin films.

4.2.1.8 Annealing of the Sb_2S_3 thin films

The annealing of Sb_2S_3 thin films is carried out using high temperature tabular furnace supplied by Taurus and Associates, Adyar, Madras in nitrogen atmosphere at temperature of 200 ^oC for 2 hours to study the effect of annealing on crystallinity of the films.

4.2.2 CHARACTERIZATION OF Sb_2S_3 THIN FILMS

The Sb_2S_3 films prepared at optimized preparative parameters were characterized by using X-ray diffraction, scanning electron microscopy, optical absorption, dark resistivity and TEP measurement techniques.

4.2.2.1 X-Ray diffraction (XRD)

XRD studies were carried out as discussed in section 3.2.2.1.

4.2.2.2 Scanning electron microscopy (SEM)

SEM studies were carried out as discussed in section 3.2.2.2.

4.2.2.3 Optical absorption

To carry out the optical absorption studies the procedure discussed in section 3.2.2.3 was adopted.

4.2.2.4 Electrical resistivity

The details of experimental set up are discussed in Section 3.2.2.4.

4.2.2.5 Thermoelectric Power (TEP)

The experimental setup for measurement of TEP is described in Section 3.2.2.5.

4.3 RESULTS AND DISCUSSION

The thickness of the prepared film was determined using relation 2.1 by weight difference method using the density of the deposited material as 4.1 gm / cm^3 , same as that of bulk material. The thickness was found to be 0.5 μm.

4.3.1 X - ray diffraction (XRD)

The Sb_2S_3 compound was analyzed with the help of XRD patterns. Fig. 4.1 shows the XRD patterns for both as deposited and annealed films. It shows a single well defined peak in the direction of plane (060) [d = 1. 8894 Å] for as deposite films. The orientations along (310), (111), (211), (221), and (301) planes, having XRD peak intensity (I/Imax) < 5%, have also been observed. The observed '*d*' values of Sb_2S_3 films match with the standard '*d*' values [21] of Sb_2S_3 which confirms the formation of Sb_2S_3 . The observed and

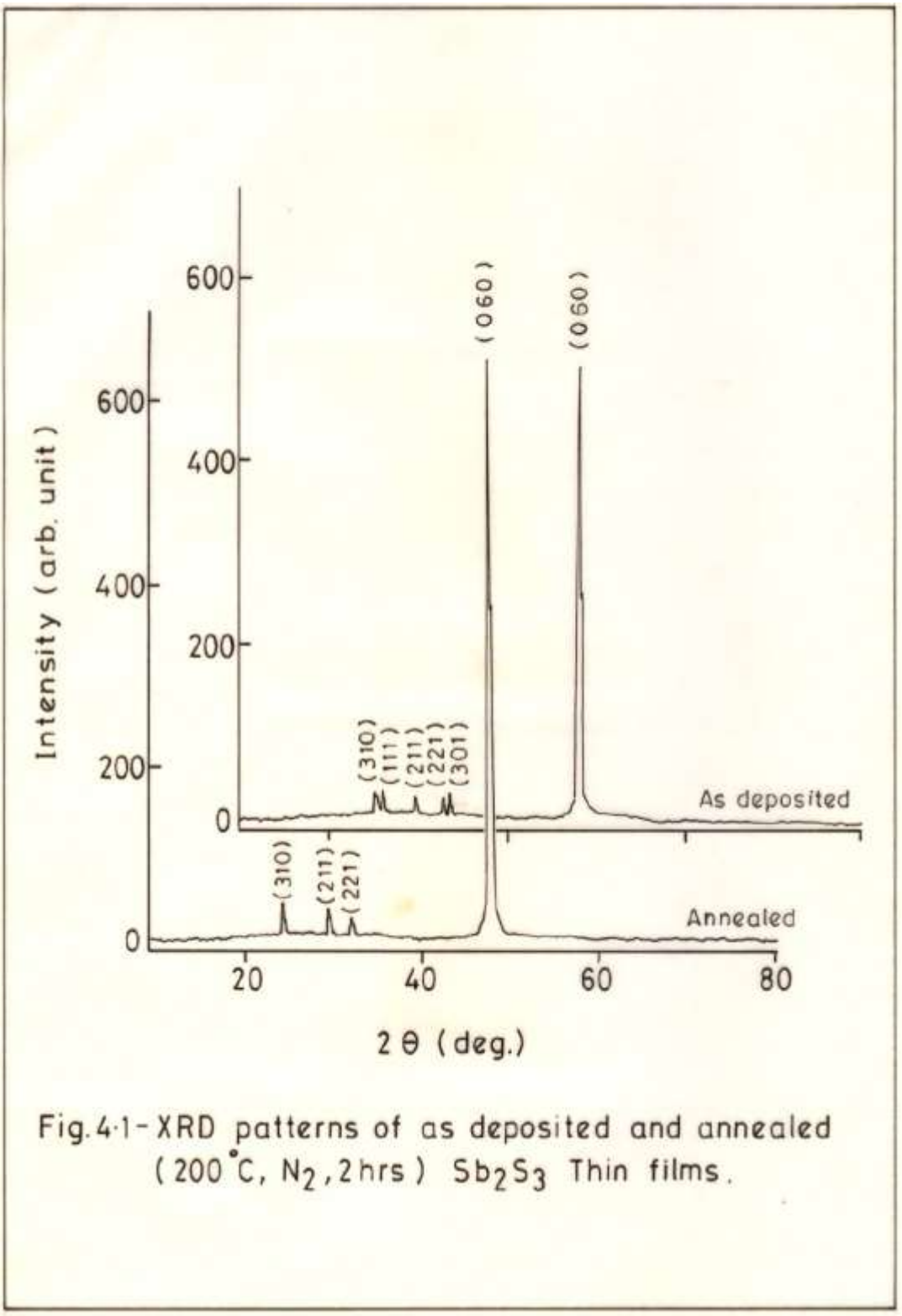

Fig. 4·1 - XRD patterns of as deposited and annealed (200 °C, N_2, 2 hrs) Sb_2S_3 Thin films.

standard *d* values are listed in Table 5.1. The lattice parameters a_0 , b_0 , c_0 are calculated for orthorhombic structure of Sb_2S_3 films. The calculations lead to a_0 = 11.1844 (std. 11.299 Å), b_0 = 11.33532 (std. 11.131 Å) and c_0 = 3.8353 Å (std. 3.839 Å) [22].

Sr. No.	Observed *d* (Å)	Standard *d* (Å)	I / Io (%)	(*hkl*) planes
1.	3.5414	3.556	5.07	(310)
2.	3.4802	3.458	4.17	(111)
3.	2.9864	3.053	2.30	(211)
4.	2.7631	2.764	1.45	(221)
5.	2.7098	2.680	2.34	(301)
6.	1.8894	1.865	100.00	(060)

In order to study the grain size of the Sb_2S_3 thin films, films have been studied by taking slow- scan XRD pattern around the (060) peak with a step width of the diffractometer to be 0.02 (2θ) min^{-1}. The grain size is calculated by using the Scherrer's relation

$$d = \lambda / D \cos\theta \qquad (4.1)$$

Where D is the full width at half maximum of the peak and λ = 1.5418 Å is the wavelength with Cu -Kα target. The grain size is found to be 321 Å.

4.3.2 Scanning electron microscopy (SEM)

The surface morphology of the Sb_2S_3 thin film was studied by SEM micrographs. SEM micrographs of Sb_2S_3 films at three different magnifications (5,000x , 10,000x and 20,000x) are shown in Fig. 4.2. The micrograph at 5,000x (Fig. 4.2 (a)) shows that the film deposited covers the whole substrate with almost an even morphology. The micrographs of the same film at magnifications 10,000x and 20,000x (Fig. 4.2 (b & c)) show the uneven surface morphology with random distribution of over growth particles. The films surface is rough and shows the presence of extra particles.

4.3.3 Optical absorption

The optical absorption studies were carried out in the wavelength range of 350 to 850 nm. The variation of optical density (α t) with wavelength (λ) is depicted in Fig. 4.3. It shows that the optical absorption coefficient 'α' is a function of photon energy [23]. The absorption coefficient is found to be of the order of 10^4 cm^{-1} indicating the presence of a direct band edge [24]. Following the usual theoretical analysis, the energy dependent absorption coefficient can be expressed by the relation 2.8 for allowed direct transition with n = 1/2. The large values of α (10^4 - 10^6 cm^{-1}) corresponding to photon energies near a band edge lead to a direct transition which has already been reported for Sb_2S_3 material [15,25-26].

The absorption of photon energy for Sb_2S_3 thin films have been explained by many workers. In present case the measurements are carried out

a)

b)

c)

Fig. 4.2 : SEM micrographs for Sb_2S_3 thin films prepared from non-aqueous medium at magnifications a) 5000x, b)10000x and 20000x

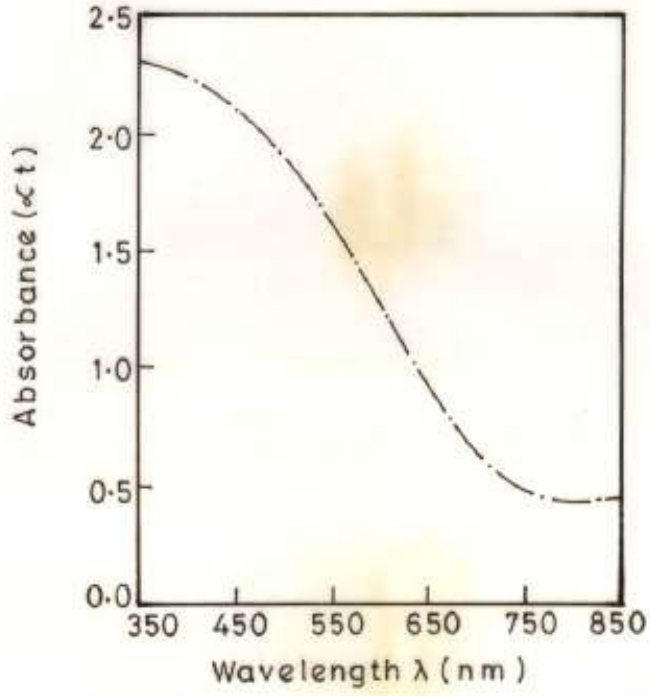

Fig. 4·3 – Variation of optical density (absorbance) with wavelength for Sb_2S_3 thin film.

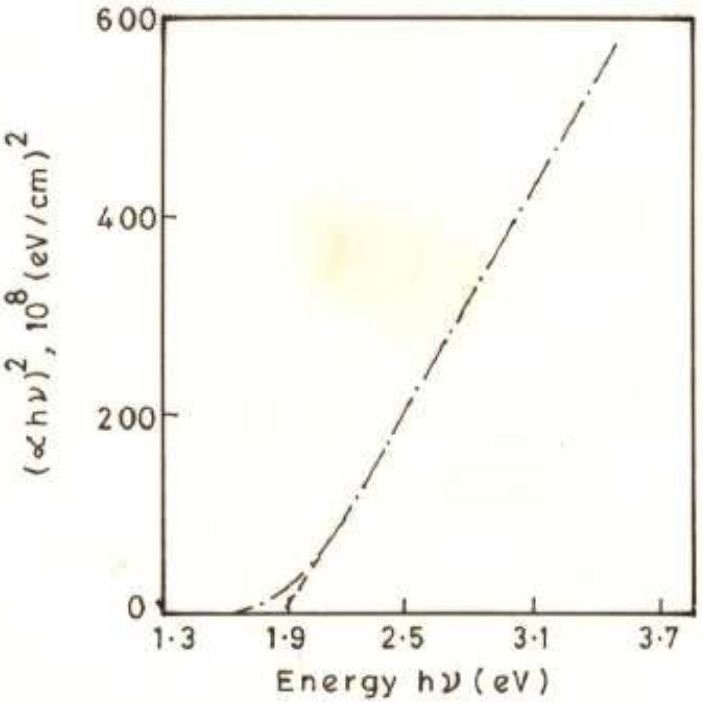

Fig. 4·4 – Plot of $(\alpha h\nu)^2$ against $h\nu$ for Sb_2S_3 thin film.

at room temperature where the absorption will be due to a band to band transition as the excitation band is not likely to be present . This is confirmed by plotting $(\alpha h\nu)^2$ versus $h\nu$ as shown in Fig. 4.4. The plot is straight line indicating that the direct transition is the dominant transition involved. The energy gap of 1.8 eV is obtained by extrapolating the linear portion of the plot to energy axis at $\alpha = 0$. This value is in good agreement with a value reported earlier [11, 13, 25] for thin films of Sb_2S_3.

4.3.4 Electrical resistivity

Two point d.c. dark resistivity measurement shows that the prepared Sb_2S_3 films are highly resistive. The room temperature dark resistivity is of the order of 10^6-10^7 Ω.cm, similar to the results of others [12 - 13, 16]. The high resistivity of the film may be due to discontinuities, large grain boundaries and low thickness of the film. The electrical resistivity and thermal activation energies have been estimated using relation 2.4 for resistivity. The variation of log (ρ) with reciprocal of temperature is depicted in Fig. 4.5. It is seen that the resistivity decreases with increase in temperature and supports for the semiconducting nature of the Sb_2S_3 thin films. From the slope of log (ρ) versus 1/T plot, the value of activation energy was calculated. The observed activation energy for the film is 0.87 eV. For perfectly stoichiometric Sb_2S_3 [27] crystal, a activation energy of 0.9 eV has been observed. These results supports the formation of perfectly or nearly stoichiometric spray deposited Sb_2S_3 material, from non-aqueous medium.

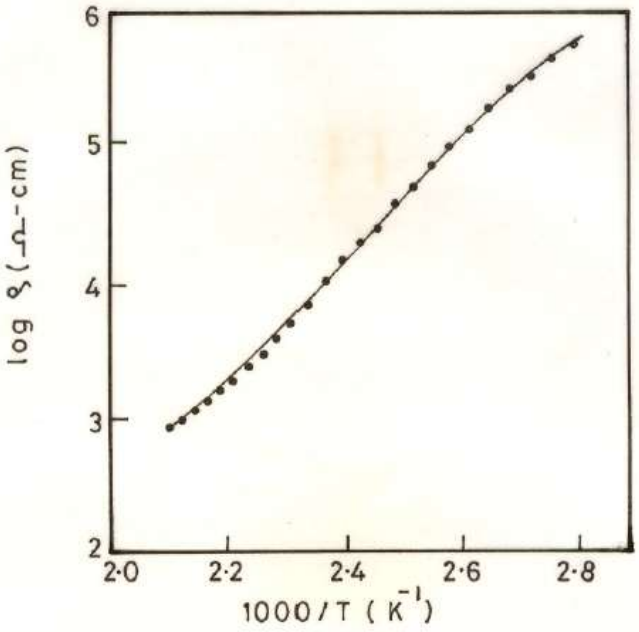

Fig. 4·5 – Variation of log ρ with 1000/T for Sb_2S_3 thin film.

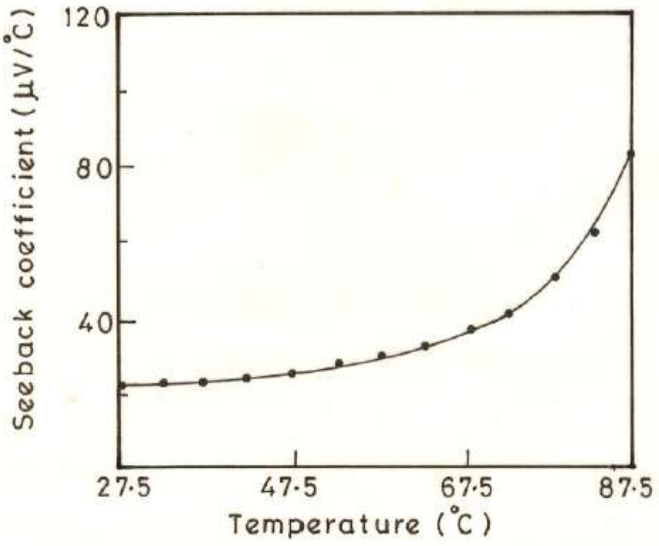

Fig. 4·6 – Variation of seeback coefficient against the mean temperature for Sb_2S_3 thin film.

4.3.5 Thermoelectric power (TEP)

The thermoelectric power measurements were used to evaluate Seebeck coefficient and nature of the material being studied . The dependence of TEP on temperature is depicted in Fig. 4.6. It is seen that the polarity of thermally generated voltage for Sb_2S_3 films prepared from non-aqueous medium is positive towards hot end, indicating the Sb_2S_3 is n-type in nature. The plot shows that increase in temperature results in the increase in TEP above the mean temperature of 50 ^oC. This is attributed to the increase in carrier concentration and mobility of charge carriers with rise in temperature.

4.3.6 Annealing of Sb_2S_3 thin films

Annealing of Sb_2S_3 thin films is carried out at temperature 200 ^0C in nitrogen atmosphere for 2 hours to study the effect on crystallinity and the grain size of thin films. It is seen that the intensity of (060) plane increases, as shown in Fig. 4.1, after annealing. The increase in grain size from 321Å to 350Å has been observed. The calculated values of lattice parameters of annealed Sb_2S_3 thin films are 11.2899, 11.3334 and 3.8132 Å respectively. These values are very much close to the values reported for single crystal Sb_2S_3 [22] . The change in the values of lattice parameters after annealing may be due to increase in grain size. Annealing promotes fusion of small crystallites (agglomerisation) thus reducing the grain boundary area, leads to the increase in grain size of the Sb_2S_3 particles.

REFERENCES

1. J.R.Lince, J. Mater. Res., 5 (1990) 218.
2. K.C.Mandal and O. Savadogo, J. Mat. Chem., 1 (1991) 301.
3. C.D. Lokhande, Mat. Chem. Phys., 27 (1991) 1.
4. D. Cope, U.S. patent No. 2875, 359 (1959).
5. J. Grigas, J. Meshkaskas and A. Orliukas, phys. stat. sol. (a), 37 (1976) K39.
6. M.S. Ablowa, A.A. Andreev, T.T. Dedegkaev, B.T. Melekh, A.B. Pevtsov, N.S. Sheridal and L.N. Shumilova, Sov. Phys. Semicond., 10 (1976) 629.
7. M.J. Chokalingam, K. Nagraja Rao, N. Rangarajan and C.V. Suryanarayana, J. Phys. D : Appl. Phys., 3 (1970) 1641.
8. E. Montrimass and A. Pazera, Thin Solid Films, 34 (1976) 65.
9. J. George and M.K. Radhakrishnan, Solid State Commun., 33 (1980) 987.
10. P. Arun, A.G. Vedeshwar and N.C. Mehra, Mater. Res. Bull., 32 (1997) 907.
11. O. Savadogo and K.C. Mandal, Sol. Ener. Mater. Solar Cells, 26 (1992) 117 and J. Electrochem. Soc., 141 (1994) 2871.
12. C.D. Lokhande, Mater. Chem. Phys., 28 (1991) 145.
13. J.D. Desai and C.D. Lokhande, Bull. Electrochem., 9 (1993) 242.
14. S.H. Pawar, S. Tamhankar, P.N. Bhosale and M.D. Uplane, Ind. J. Pure and Appl. Phys., 21 (1983) 665.

15. L.D. Deshmukh, S.G. Holikatti, B.P. Rane, M.I. Bele and P.P. Hankare, Bull. Electrochem., 9 (1993) 237.

16. C.H. Bhosale, M.D. Uplane, P.S. Patil and C.D. Lokhande, Thin Solid Films, 248 (1994) 137.

17. N.S. Yesugade, C.D. Lokhande and C.H. Bhosale, Thin Solid Films, 263 (1995) 145.

18. K.Y. Rajpure, C.D. Lokhande and C.H. Bhosale, Mat. Chem. Phys., 51 (1997) 252.

19. K.Y. Rajpure, C.D. Lokhande and C.H. Bhosale J. Phys. Chem. Solids, (Revised Submitted) (1999).

20. A.A. Mostovskii, L.G. Timofeev and O.A. Timofeev, Sov. Phys - Solid State, 6 (1964) 389.

21. A.S.T.M. diffraction data file card No. 6-0474.

22. R.W.G. Wyckoff, Crystal Structures, Vol. 2, Willy and Sons, New York, (1964).

23. E. Shanti, V. Dutta, A. Banerjee and K.L. Chopra, J. Appl. Phys., 51 (1980) 6243.

24. T.S. Moss, in Optical Properties of Semiconductors', Butterworths (London), (1961), p.37.

25. C. Ghosh and B.P. Verma, Solid State Commun., 31 (1979) 683.

26. O. Savadogo and K.C. Mandal, J. Electrochem. Soc.,139 (1992) L-16.

27. A. Karpus, I.V. Bataranas and M. Mikalkevicius, Lietuvos TSR Aukstosius Mokyklos, 2 (1962) 289.